Interleaved dual buck converters with low current ripple for green hydrogen production

Diego Concha, Ana M Llor, Hugues Renaudineau, Maurice Fadel, Henri Schneider, Javier Solano, Samir Kouro

Interleaved Dual Buck Converters With Low Current Ripple for Green Hydrogen Production

Diego Concha[1] , Ana M. Llor[1,2], Hugues Renaudineau[2], Maurice Fadel[1], Henri Schneider[1], Javier Solano[3], Samir Kouro[2]*

[1]*Université de Toulouse, LAPLACE CNRS-INPT-UPS, Toulouse, France*
[2]*Department of Electronic Engineering, Universidad Tecnica Federico Santa Maria, Valparaiso, Chile*
[3]*EIFER - European Institute for Energy Research, Karlsruhe, Germany*
**E-mail: diego.concha-fuentes@laplace.univ-tlse.fr*

Abstract

In this paper, interleaved dual buck converters are analyzed for use with electrolyzers coupled to renewable energy sources. The topology offers advantages such as low blocking voltage stress, and the possibility to reach high current for large electrolyzers through interleaved connection of converter channels. Additionally, interleaved dual buck converters can generate points of current ripple cancellation for a discrete number of output voltage values, which increase as more channels are connected in interleaved mode. This can lead to a reduction in the power of each channel and extend the lifespan of the electrolyzer. The theoretical analysis of the converter and the dependence of the output current ripple on the different system variables and parameters are addressed. Simulation results are presented for a 6-channel interleaved configuration for a $1MW$ nominal power operating point, which can be reconfigured to 5 channels in order to reduce the output current ripple.

1 Introduction

Low-carbon hydrogen, also known as green hydrogen is emerging as an important energy vector and feedstock for energy transition applications such as fuel cell-powered transportation systems [1], hydrogen combustion [2], hydrogen energy storage systems [3], and hydrogen-based synthetic fuels production [4]. Low-carbon hydrogen is produced from water electrolysis using renewable energy sources such as wind and photovoltaic power [5]. Consequently, power converters are essential for these applications, as high-power electrolyzers are powered with high DC currents and operate at low voltage.

There are different electrolyzer technologies including the Proton Exchange Membrane (PEM), Alkaline Water Electrolyzer (AWE), and Solid Oxide Electrolyzer (SOEC) [6]. For a better response to power fluctuations - an intrinsic characteristic of renewable energy sources - PEM is the most adequate alternative [7], which is considered in this work. Water electrolyzers can be connected either through AC coupling to the AC grid using a rectifier for single-stage configurations or a rectifier followed by a DC-DC converter for a two-stage solution. For DC coupling to DC grids, photovoltaic energy systems, and the DC-link of wind turbines, only DC-DC converters are needed. Hence, in most cases, high current DC-DC converters are required for this application. These converters usually operate in buck mode since DC grids and DC links of renewable energy conversion systems operate at $1000V$ or $1500V$, while electrolyzers typically range from $200V$ to $500V$ at large-scale applications. A high-voltage conversion ratio, with low output voltage and reduced current ripple are the main requirements to be considered for DC-DC converters feeding electrolyzers [8]. Isolated and non-isolated converters have already been proposed [9]. The choice of a particular converter topology can save cost, reduce size, increase efficiency, and improve reliability, all of which can impact the levelized cost of hydrogen [10].

Within non-isolated converter candidates, the classic buck converter has been considered the most straightforward solution [11]. Simple, low cost, easy to control, and a reduced number of components make this converter a suitable candidate. However, the industry trend to elevate the DC-bus voltages to reduce DC currents and thereby increase efficiency can be an issue for this traditional converter, since its power switch and diode block the entire input voltage, and will require operating within a reduced range of duty cycles to achieve the high input-output voltage conversion ratio. One solution is the voltage divider converter principle, where semiconductors block a fraction of the input voltage of the DC-DC converter, usually lower than the input voltage, allowing the use of switches with lower voltage ratings [12], [13].

Due to the high input-output voltage ratio and blocking voltage stress on devices, another challenge is to increase the power level of both electrolyzers and power converters used to supply DC currents to them. The use of interleaved DC-DC converters is a natural way to reach higher power levels, while simultaneously reducing the output current ripple. This is considered advantageous for increasing the electrolyzer lifespan [14].

The dual buck converter has been proposed in [15] as an advancement over traditional buck converters, particularly in reducing electrical stress. In [16], it is suggested for high-power applications through the utilization of two channels in an interleaved configuration. Addressing hydrogen production applications, [17] discusses a control strategy involving a two-channel dual buck converter for connecting a DC grid to a PEM electrolyzer. Additionally, [18] presents a dual buck converter topology with multi-output capability tailored for multiple stacks of electrolyzers.

https://doi.org/10.1049/icp.2024.2213

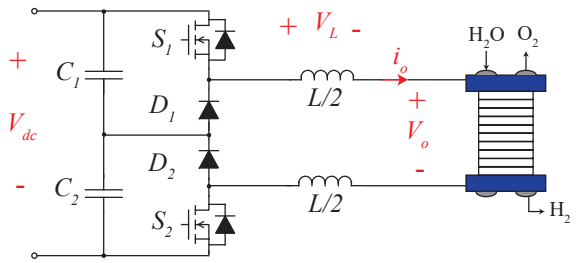

Fig. 1 Proposed dual buck converter for hydrogen production application.

This paper presents the use of interleaved dual buck converters to power PEM electrolyzers. The dual buck converter reduces the blocking voltage of power semiconductors to half of the input voltage, allowing operation with higher input DC-bus voltages. In addition, the use of several interleaved channels is analyzed to assess the impact on the output current ripple and positively affect the lifespan of the electrolyzer.

The paper is organized as follows: in section 2, the converter model is discussed. In section 3, the interleaved connection of the topology is analyzed, including the dependence of the output current ripple on the system parameters and variables. The model of the electrolyzer is addressed in section 4. Simulation results are presented in section 5 to validate the theoretical analysis. Finally, concluding remarks are given in section 6.

2 Dual buck converter model

Fig. 1 shows the power circuit topology of the proposed DC-DC converter. To achieve symmetry in the converter topology, the total inductance L is divided into $L/2$ between positive and negative terminals. Due to the input connection of capacitors C_1 and C_2, the four semiconductors will only block half of the input voltage V_{dc}.

Fig. 2 shows the dual buck converter operating modes when duty cycle $D < 0.5$. The gate signals S_1 and S_2 are phase-shifted by $180°$ relative to each other. When S_1 is turned on, the voltage across the total inductance L is:

$$\frac{V_{dc}}{2} - V_o = L\frac{\Delta i_o}{DT} \tag{1}$$

where V_{dc} is the input voltage (considered fixed for this study), V_o is the electrolyzer voltage, T is the period (inverse of the switching frequency f) and Δi_o is the electrolyzer current ripple. When both S_1 and S_2 are turned off, the voltage across the total inductance L can be expressed as:

$$V_o = L\frac{\Delta i_o}{T(\frac{1}{2} - D)} \tag{2}$$

By combining (1) and (2), leads to the converter input-output voltage transfer function:

$$V_o = DV_{dc} \tag{3}$$

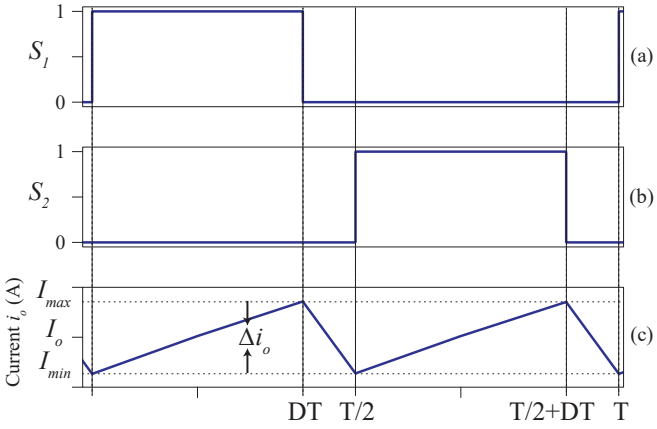

Fig. 2 Dual buck converter operating modes when $D < 0.5$. (a) switching signal S_1. (b) switching signal S_2. (c) electrolyzer current i_o.

It is worth noting that the operating modes when $D > 0.5$ are not analyzed, as they fall outside the operational range of the application. For this study, the duty cycle range comprises values from $0.25 < D < 0.4$, corresponding to an output voltage range $375V < V_o < 600V$, for a $V_{dc} = 1500V$.

3 Interleaved connection

For large-scale industrial electrolyzers, high currents in the order of several kilo-amps are required. Therefore, the interleaved connection of DC-DC converters is an appropriate solution to reduce the electrical stress in all converter components, especially in semiconductors [19]. The electrolyzer current i_o is equally shared among the interleaved channels, denoted as n. Depending on the number of channels, zero total output current ripple can be achieved for specific duty cycles or output voltage values [20], which is advantageous for the lifespan of the electrolyzer [21], [22]. Moreover, interleaved connection improves the system reliability in case one or more channels fail, due to inherent redundancy.

Fig. 3 shows the interleaved dual buck converters topology with n channels, where i_{L1} is the inductor current of the first channel, i_{L2} is the inductor current of the second channel, and so

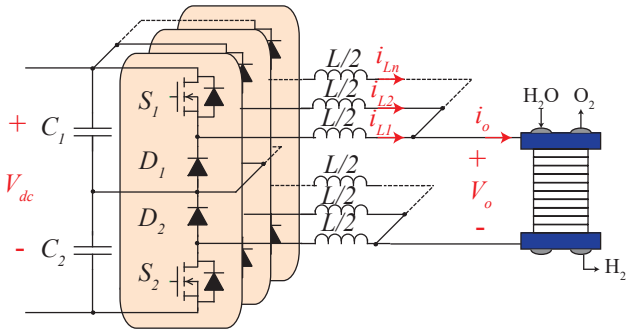

Fig. 3 Interleaved dual buck converters topology with n channels.

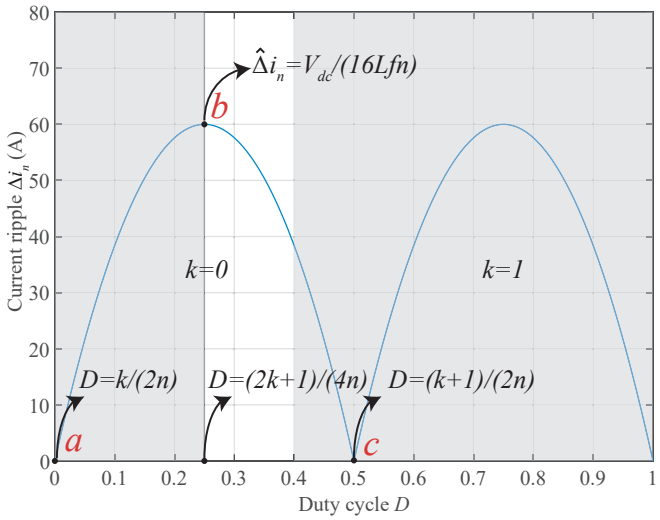

Fig. 4 Current ripple Δi_n vs duty cycle D in dual buck converters.

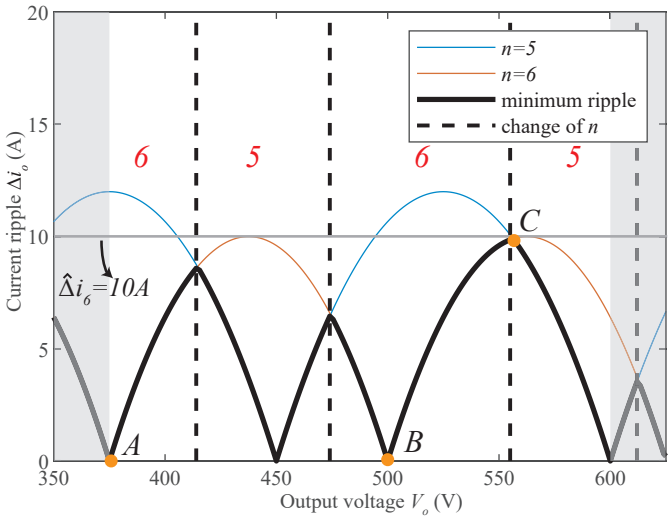

Fig. 5 Electrolyzer current ripple Δi_o vs output voltage V_o for $n = 5$ and $n = 6$ at $V_{dc} = 1500V$. The red numbers represent the optimal number of interleaved channels for ripple minimization. The point B is the nominal operational point with $n = 6$.

on up to i_{Ln}, depending on the number of interleaved channels. In this study, an interleaved configuration of 6 channels is considered, which is then reconfigured to 5 to validate the theoretical analysis through simulations.

3.1 Current ripple in interleaved dual buck converters

In a single-channel dual buck converter, the current ripple Δi_o can be found according Eq. (1). For the numerical calculation of the current ripple Δi_n with n channels connected, a parameter k is defined, representing the discrete number of parabolas according to the number of channels and duty cycle, following the methodology outlined in [23]. The parameter k takes discrete values from $k \in [0, \ldots, 2n-1]$. Fig. 4 illustrates the current ripple Δi_n as a function of the duty cycle D. The shaded areas represent operating points that fall outside the range suitable for electrolyzer operation.

For $n = 1$, the maximum current ripple $\hat{\Delta} i_1$ is reached at $D = 1/4$ given by:

$$\hat{\Delta} i_1(D = 1/4) = \frac{V_{dc} \cdot \frac{1}{4}\left(\frac{1}{2} - \frac{1}{4}\right)}{Lf} = \frac{V_{dc}}{16Lf} \tag{4}$$

Consequently, the maximum current ripple $\hat{\Delta} i_n$ can be defined, by dividing by the number of connected channels, as follows:

$$\hat{\Delta} i_n = \frac{V_{dc}}{16Lfn} \tag{5}$$

The current ripple Δi_n can be expressed by a quadratic formula, representing a parabolic relationship, given by

$$\Delta i_n = aD^2 + bD + c \tag{6}$$

Considering three points a, b and c as depicted in Fig. 4, a system of three equations is established:

$$\begin{cases} a\left(\frac{k}{2n}\right)^2 + b\left(\frac{k}{2n}\right) + c = 0 \\ a\left(\frac{2k+1}{4n}\right)^2 + b\left(\frac{2k+1}{4n}\right) + c = \frac{V_{dc}}{16Lfn} \\ a\left(\frac{k+1}{2n}\right)^2 + b\left(\frac{k+1}{2n}\right) + c = 0 \end{cases} \tag{7}$$

Upon solving the system, the values of the three unknowns a, b, and c are determined to be:

$$a = \frac{-V_{dc}n}{Lf} \tag{8}$$

$$b = \frac{V_{dc}(2k+1)}{2Lf} \tag{9}$$

$$c = \frac{-V_{dc}k(1+k)}{4Lfn} \tag{10}$$

Finally, the current ripple in interleaved dual buck converters is:

$$\Delta i_n = \frac{-V_{dc}n}{Lf}D^2 + \frac{V_{dc}(2k+1)}{2Lf}D - \frac{V_{dc}k(1+k)}{4Lfn} \tag{11}$$

where:

$$\frac{k}{2n} < D < \frac{k+1}{2n} \tag{12}$$

Given that the output voltage V_o is the product of the duty cycle D and the constant input voltage V_{dc}, the electrolyzer current ripple Δi_o can be expressed in terms of V_o, as illustrated in Fig. 5. The black-highlighted curve represents the minimization of the total current ripple, while the vertical dashed lines correspond to the output voltage points at which this minimized curve changes based on the number of activated channels. For example, within the range from $V_o = 415V$ to $V_o = 474V$, minimum ripple will be obtained for 5 channels,

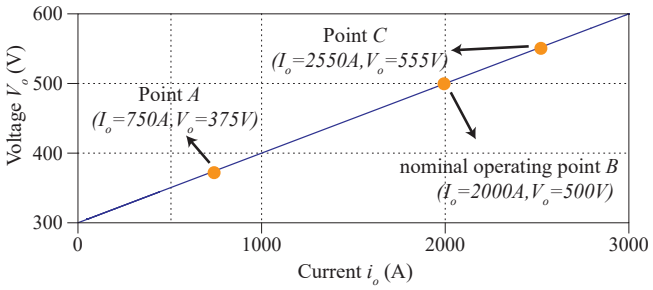

Fig. 6. Electrolyzer characteristic curve.

while from $V_o = 475V$ to $V_o = 554V$, activating 6 channels is preferable. Within the operating range of output voltage, the maximum output ripple is $\hat{\Delta}i_6 = 10A$, observed at point C. Notably, specific output voltage levels exhibit points of current ripple cancellation. Designing the system to operate at these points would be ideal for mitigating output current ripple. For this analysis, the nominal point is located at point B, with $V_o = 500V$.

4 Electrolyzer Model

Several equivalent circuit models have been proposed for PEM electrolyzers, considering both dynamic and static operations to represent the electrochemical effects of the device [21]. Fig. 6 illustrates the static curve of the implemented electrolyzer equivalent model, which is implemented using a voltage source in series with a resistance, denoted as V_{oc} and R_s, respectively. Assuming a constant input voltage V_{dc}, the varying power harvested from solar or wind energy will shift the operating point of the electrolyzer along its polarization curve.

Due to physical and chemical processes occurring within the electrolyzer, such as proton diffusion across the membrane or mass and heat transport phenomena, the typical response time in the dynamics of a PEM electrolyzer can range from seconds to minutes [24]. On the contrary, power converters often operate at much higher frequencies, ranging from kilohertz to even megahertz levels, depending on the type of converter. It is for this reason that a static electrolyzer model is used to simplify the analysis without significantly sacrificing precision.

While electrolyzers typically operate at relatively low voltages, typically under $1000V$, the industry trend is towards increasing power capacity, often achieved by increasing the number of cells in series. For the simulation model of a $1MW$ PEM electrolyzer, an output voltage of $500V$ is considered, in accordance with typical specifications for PEM electrolyzer stacks [25].

5 Simulation results

Table 1 summarizes the simulation parameters considered in this work. For all simulations input voltage is considered fixed at $V_{dc} = 1500V$. For the design of inductor L, a maximum ripple of $\hat{\Delta}i_6 = 10A$ is considered for $n = 6$ as expressed by Eq. (5).

Table 1 Simulation parameters.

Parameter	Symbol	Value
Nominal output power	P_o	$1MW$
Nominal output voltage	V_o	$500V$
Nominal output current	I_o	$2kA$
Nominal input voltage	V_{dc}	$1500V$
Electrolyzer resistance	R_s	0.1Ω
Electrolyzer voltage source	V_{oc}	$300V$
Switching frequency	f	$10kHz$
Inductor	L	$156.25\mu H$

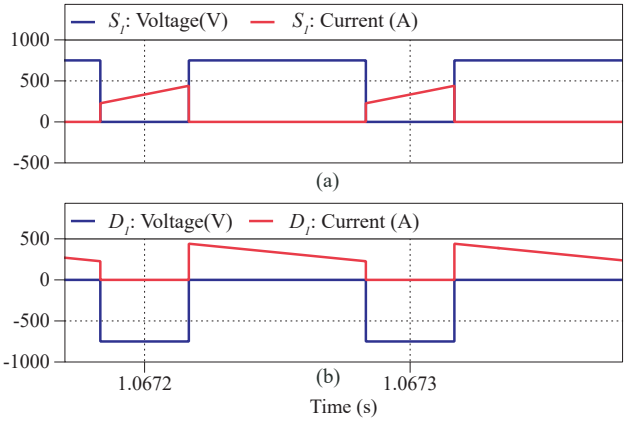

Fig. 7 Semiconductors waveforms for $n = 6$ at nominal operating point B. (a) S_1 voltage and current. (b) D_1 voltage and current.

Fig. 7 illustrates the waveforms of the power switch S_1 and diode D_1 for $n = 6$ at the nominal operating point B. These curves depict voltages and currents of a single channel, with similar characteristics for the other five channels, though shifted in time. It is evident that the maximum voltage, depicted in blue, reaches half of the nominal input voltage V_{dc}, which is $750V$.

Fig. 8 illustrates the total output current and the individual inductor currents of each interleaved channel when $V_o = 375V$, corresponding to point A in Fig. 5. As observed, this point represents a cancellation of the current ripple, achieved by activating 6 interleaved channels, with an average output current of $750A$ and a significantly reduced ripple. If the output voltage remains within the range of $375V$ to $415V$, there is no need to change the operative channels to minimize the output current ripple.

Fig. 9 depicts the scenario where $V_o = 500V$, representing the nominal operating point B corresponding to an electrolyzer power of $1MW$. Similar to point A, the output current exhibits no ripple as it aligns with one of the cancellation points for the $n = 6$ channel configuration. Within the output voltage range of $475V$ to $554V$, the total current ripple is minimized by utilizing 6 channels.

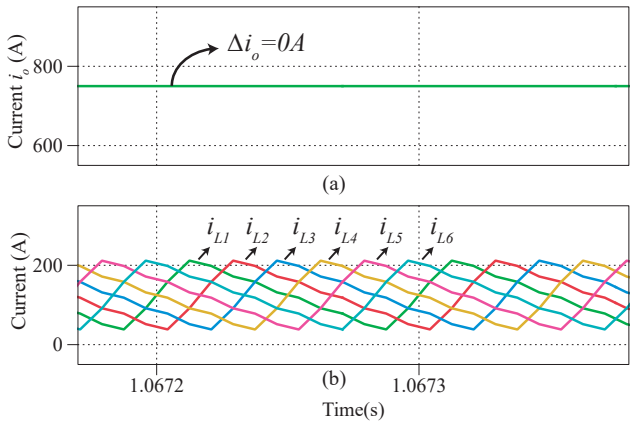

Fig. 8 Waveforms with 6 channels at $V_o = 375V$ (point A). (a) output current. (b) inductors currents.

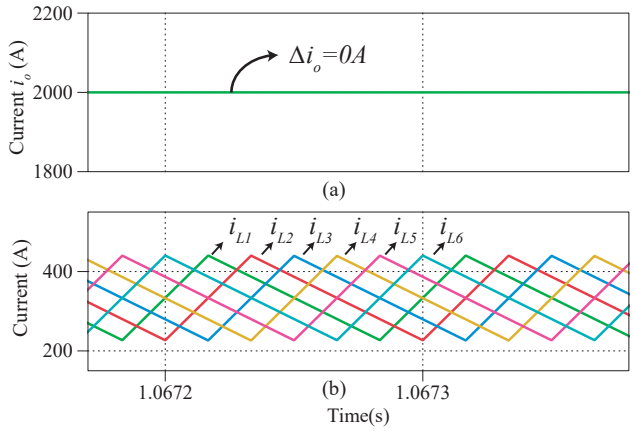

Fig. 9 Waveforms with 6 channels at $V_o = 500V$ (nominal point B). (a) output current. (b) inductors currents.

Fig. 10 illustrates the same variables when $V_o = 555V$, corresponding to point C in Fig. 5. By activating 6 channels, the current ripple may not be adequately reduced for output voltages greater than or equal to 555V, potentially affecting the lifespan of the electrolyzer. Optimal ripple reduction, achieving a value of $\Delta i_o = 10A$ as depicted in Fig. 5, is attained by activating only 5 channels. Specifically, this $\Delta i_o = 10A$ represents the maximum achievable ripple ($\hat{\Delta} i_6$) within the operating range of $375V$ to $600V$, constituting 0.39% of the average output current at this operating point, where the average output current is $2550A$.

The interleaved dual buck converters offers ample flexibility to reconfigure and operate the system while minimizing current ripple. This adaptability is facilitated by the number of interleaved channels activated.

6 Conclusion

This paper proposes interleaved dual buck converters as a suitable topology for use in a low-carbon hydrogen production

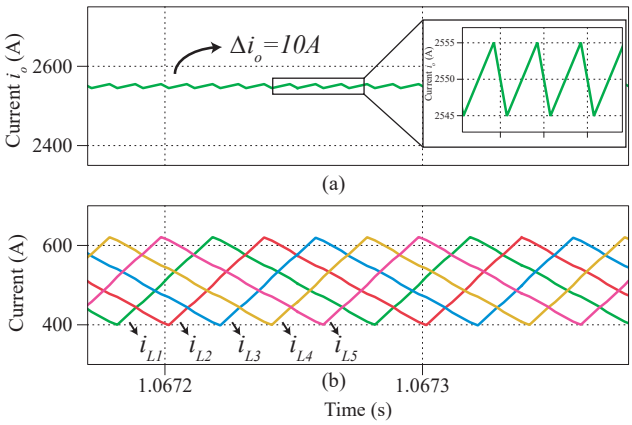

Fig. 10 Waveforms with 5 channels at $V_o = 555V$ (point C). (a) output current (b) inductors currents.

system. This configuration achieves a halving of the blocking voltage stress on semiconductors compared to the input voltage. The interleaved connection enables higher current levels to be reached and reduces current ripple.

To evaluate the topology, a 6-channel interleaved configuration is utilized, which is then reconfigured to 5 channels to reduce the output current ripple and extend the lifespan of the electrolyzer. For discrete output voltage values, the current ripple can be reduced to zero depending on the number of activated channels in interleaved mode.

Acknowledgements

This work was supported in part by the following projects from the Agencia Nacional de Investigacion y Desarrollo (ANID): AC3E (ANID/Basal/FB0008), FONDECYT Iniciacion grant 11240917, and SERC Chile (ANID/FONDAP/1523A0006). The work was also supported by the European Institute for Energy Research. These contributions are gratefully acknowledged.

7 References

[1] N. Shakeri, M. Zadeh, and J. Bremnes Nielsen, "Hydrogen fuel cells for ship electric propulsion: Moving toward greener ships," *IEEE Electrification Magazine*, vol. 8, no. 2, pp. 27–43, 2020.

[2] E. Giacomazzi, G. Troiani, A. Di Nardo, G. Calchetti, D. Cecere, G. Messina, and S. Carpenella, "Hydrogen combustion:features and barriers to its exploitation in the energy transition," 09 2023.

[3] J. Li, G. Li, S. Ma, Z. Liang, Y. Li, and W. Zeng, "Modeling and simulation of hydrogen energy storage system for power-to-gas and gas-to-power systems," *Journal of Modern Power Systems and Clean Energy*, vol. 11, no. 3, pp. 885–895, 2023.

[4] V. Ram and S. R. Salkuti, "An overview of major synthetic fuels," *Energies*, vol. 16, no. 6, 2023.

[5] IEA, "Global hydrogen review 2023," Paris, 2023, licence: CC BY 4.0.

[6] M. Mohebali Nejadian, P. Ahmadi, and E. Houshfar, "Comparative optimization study of three novel integrated hydrogen production systems with soec, pem, and alkaline electrolyzer," *Fuel*, vol. 336, p. 126835, 2023.

[7] S. Shiva Kumar and V. Himabindu, "Hydrogen production by pem water electrolysis – a review," *Materials Science for Energy Technologies*, vol. 2, no. 3, pp. 442–454, 2019.

[8] D. Guilbert, S. M. Collura, and A. Scipioni, "Dc/dc converter topologies for electrolyzers: State-of-the-art and remaining key issues," *International Journal of Hydrogen Energy*, vol. 42, no. 38, pp. 23 966–23 985, 2017.

[9] J. Lei, H. Ma, G. Qin, Z. Guo, P. Xia, and C. Hao, "A comprehensive review on the power supply system of hydrogen production electrolyzers for future integrated energy systems," *Energies*, vol. 17, no. 4, 2024.

[10] H. Renaudineau, A. M. Llor, R. Cortés D., C. A. Rojas, C. Restrepo, and S. Kouro, "Photovoltaic green hydrogen challenges and opportunities: A power electronics perspective," *IEEE Industrial Electronics Magazine*, vol. 16, no. 1, pp. 31–41, 2022.

[11] M. E. Şahin, H. İbrahim Okumuş, and M. T. Aydemir, "Implementation of an electrolysis system with dc/dc synchronous buck converter," *International Journal of Hydrogen Energy*, vol. 39, no. 13, pp. 6802–6812, 2014.

[12] L. Costa, S. Mussa, and I. Barbi, "Multilevel buck dc-dc converter for high voltage application," 11 2012, pp. 1–8.

[13] A. Ganjavi, H. Ghoreishy, and A. A. Ahmad, "A novel single-input dual-output three-level dc–dc converter," *IEEE Transactions on Industrial Electronics*, vol. 65, no. 10, pp. 8101–8111, 2018.

[14] H. Buitendach, R. Gouws, C. Martinson, C. Minnaar, and D. Bessarabov, "Effect of a ripple current on the efficiency of a pem electrolyser," *Results in Engineering*, vol. 10, p. 100216, 03 2021.

[15] X. Ruan, B. Li, and Q. Chen, "Three-level converters-a new approach for high voltage and high power dc-to-dc conversion," in *2002 IEEE 33rd Annual IEEE Power Electronics Specialists Conference. Proceedings (Cat. No.02CH37289)*, vol. 2, 2002, pp. 663–668 vol.2.

[16] M. Ilic, B. Hesterman, and D. Maksimovic, "Interleaved zero current transition three-level buck converter," in *Twenty-First Annual IEEE Applied Power Electronics Conference and Exposition, APEC*, 2006.

[17] B. Yodwong, D. Guilbert, W. Kaewmanee, M. Phattanasak, M. Hinaje, and G. Vitale, "Modified sliding mode-based control of a three-level interleaved dc-dc buck converter for proton exchange membrane water electrolysis," in *2021 Research, Invention, and Innovation Congress: Innovation Electricals and Electronics (RI2C)*, 2021, pp. 221–226.

[18] S. Udomkaew, W. Saksiri, K. Sengsui, M. Phattanasak, R. Gavagsaz-Ghoachani, and s. Pierfederici, "Modular-three-level buck converter for electrolyzer applications: current control with capacitors voltage balancing control," 11 2023, pp. 1–5.

[19] V. Guida, D. Guilbert, and B. Douine, "Literature survey of interleaved dc-dc step-down converters for proton exchange membrane electrolyzer applications," *Transactions on Environment and Electrical Engineering*, vol. 3, p. 33, 03 2019.

[20] J. Duan, S. Wang, Y. Xu, S. Fan, K. Zhao, and L. Sun, "Variable multiple interleaved bi-directional dc/dc converter with current ripple optimization," *Applied Sciences*, vol. 13, no. 3, 2023.

[21] B. Yodwong, D. Guilbert, M. Hinaje, M. Phattanasak, W. Kaewmanee, and G. Vitale, "Proton exchange membrane electrolyzer emulator for power electronics testing applications," *Processes*, vol. 9, no. 3, 2021.

[22] F. Parache, H. Schneider, C. Turpin, N. Richet, O. Debellemanière, Bru, A. T. Thieu, C. Bertail, and C. Marot, "Impact of power converter current ripple on the degradation of pem electrolyzer performances," *Membranes*, vol. 12, no. 2, 2022.

[23] D. Tran, S. Chakraborty, Y. Lan, J. Van Mierlo, and O. Hegazy, "Optimized multiport dc/dc converter for vehicle drivetrains: Topology and design optimization," *Applied Sciences*, vol. 8, no. 8, 2018.

[24] Ángel Hernández-Gómez, V. Ramirez, D. Guilbert, and B. Saldivar, "Cell voltage static-dynamic modeling of a pem electrolyzer based on adaptive parameters: Development and experimental validation," *Renewable Energy*, vol. 163, pp. 1508–1522, 2021.

[25] M. Holst, S. Aschbrenner, T. Smolinka, C. Voglstätter, and G. Grimm, "Cost forecast for low temperature electrolysis - technology driven bottom-up prognosis for pem and alkaline water electrolysis systems," 2021.